Macromolecules **2006,** *39,* 5251−5258

Control of the Density of Polymer Brushes Prepared by Surface-Initiated Atom Transfer Radical Polymerization

Zhiyi Bao, Merlin L. Bruening,* and Gregory L. Baker*

Department of Chemistry and Center for Sensor Materials, Michigan State University, East Lansing, Michigan 48824

Received January 13, 2006; Revised Manuscript Received May 24, 2006

ABSTRACT: Growth of polymer brushes from solid substrates is an attractive method for generating robust surfaces with controlled properties and functionality. This work demonstrates enhanced control over such films through variation of the areal density of the immobilized initiators used for their growth. Reaction of mercaptoundecanol monolayers on Au with both an acyl bromide initiator and a structurally similar acyl bromide diluent yields monolayers whose composition reflects the ratio of the acyl bromides in solution. Similarly, derivatization of SiO_2 with an initiator and a diluent monochlorosilane also affords control over initiator density. The thickness of polymer films grown from these modified substrates drops dramatically when the fractional coverage of the surface by initiator decreases below 10% of a monolayer because the area per polymer chain increases. However, reduced termination at low initiator coverage results in substantial increases in initiator efficiency as measured by film growth rates normalized by the fractional coverage of the surface by initiator. Variation of chain density also affords control over film swelling. Poly(2-hydroxyethyl methacrylate) films prepared with 0.1% initiator densities swell 20-fold more in water than films grown from monolayers containing only initiators. Such control should prove valuable in the use of brushes for immobilization of active, accessible biomacromolecules such as single-stranded DNA or antibodies.

Introduction

The growth of dense arrays of polymers from solid substrates represents a new and exciting approach to the modification of surfaces.[1−10] Recent advances in the growth of polymer brushes on a variety of substrates enable experiments that address the fundamental questions related to polymer brush conformations on surfaces and their response to external stimuli.[11−13] In addition, the development of diverse methods for polymer brush synthesis suggests important applications of these materials as protective coatings that exploit the high density of chains on the surface, as environmentally responsive surfaces derived from phase changes in block copolymers triggered by changes in solvent quality,[12−17] and more recently, as functional coatings.[18,19] Among the many procedures for preparing polymer brushes, atom transfer radical polymerization (ATRP) from immobilized initiators is especially attractive for its control over the molecular weight of the grafted polymers, tolerance to water and impurities, compatibility with a variety of functionalized monomers, as well as the option of carrying out polymerizations at relatively low temperatures. Moreover, because it is a controlled technique, ATRP is capable of producing thick surface-grafted polymers, binary polymers, and block copolymers.[5, 6, 8, 10, 20−25]

Along with several other methods for producing polymer brushes, ATRP yields dense polymer films, which is important for the use of these materials as anticorrosion coatings,[26−28] etch masks,[29,30] and other lithographic coatings.[29,31−33] However, in some applications, such as attachment of biomacromolecules to gene or protein chips, open films are desirable. If brushes are to be used to increase the sensitivity of sensors based on immobilized molecules, the entire brush should be available during both probe−molecule attachment and sensing. As an example,[27] poly(2-hydroxyethyl methacrylate) (PHEMA) brushes are accessible to small molecules such as perfluorooctanoyl chloride, and reaction of PHEMA with this molecule occurs in near-quantitative yield. However, when we used PHEMA brushes to initiate the ring opening polymerization of lactide to give a polymer brush having a bottle brush architecture,[34] the degree of polymerization for the lactide was only ∼6. This suggests that lactide polymerization is sterically limited and could be improved by using PHEMA brushes with lower areal densities of polymer chains. More importantly, covalent immobilization of proteins to modified PHEMA seems to occur only at the film surface, so open films will be required for depositing more than a monolayer of biomacromolecules.

This work aims at developing methods for reducing and controlling the density of polymer brushes grown from a surface using ATRP. Such control requires a technique for decreasing the areal density of active, immobilized initiators, and two basic strategies can be used for this purpose. In the first, the number of available initiators (e.g., control of initiator concentration) or the length of time the initiator solution is in contact with the surface limit the density of immobilized initiator. This strategy is difficult to apply because it requires either precise knowledge of the kinetics of the attachment reaction or fine control of a very low concentration of initiator molecules. Perhaps the most successful example of this approach is that of Genzer et al., who used an evaporation process to deposit a continuous gradient of trichlorosilane-terminated initiators on SiO_2.[35,36] Initiation of polymerization from these surfaces generated films that smoothly varied from dense brushes (full coverage of the surface by initiator) to isolated chains.[35] Similarly, Luzinov et al. employed the reaction of carboxylic acids with epoxides along with vapor-phase dosing of the carboxylic acid to control the amount of initiator anchored to glycidyl methacrylate on SiO_2.[37] Bohn et al. recently reported an electropolymerization approach to gradients of poly(acrylic acid) and poly(acrylamide) on surfaces.[38] A related strategy is to chemically activate or deactivate sites on surfaces using photochemical or scanning

---

* Corresponding authors. E-mail: bruening@msu.edu (M.L.B.); bakerg@msu.edu (G.L.B.).

10.1021/ma060095a CCC: $33.50

probe techniques,[32,39] but these methods generally are limited to flat surfaces. Analogues of this approach are photochemically or thermally initiated free radical polymerization from azo or cholorosulfonyl[40] initiators anchored on surfaces, where the number of chains initiated is related to quantum yield and half-life of the initiator. However, these methods should yield brushes with a high polydispersity.

A second strategy for controlling initiator density is to fully functionalize a surface with a mixture of the initiator and an inert analogue. Assuming both molecules have the same reactivity for the surface, it should be possible to generate an arbitrary concentration of active initiator homogeneously diluted in a matrix of inactive molecules. Advantages of this strategy include insensitivity to the kinetics of the anchoring step, the ability to cover surfaces of arbitrary size and shape, and generalization to surfaces ranging from inorganic oxides to natural materials such as cellulose. Huck et al. described the co-deposition of the ATRP initiator α-mercaptoundecyl bromoisobutyrate and undecanethiol on Au.[41] They found that initiation of the ATRP of methyl methacrylate from these surfaces gave film thicknesses that were proportional to the fraction of initiator in the self-assembled monolayer (SAM), implying constant initiator efficiency. This result is at odds with the expectation that bimolecular coupling should decrease with initiator dilution and lead to an increase in initiator efficiency. (Several studies suggest that only 1 in 10 initiators in a 100% initiator monolayer lead to polymerization.[5,20,37]) One possible explanation for this finding of constant initiator efficiency is that the two thiols phase separated to give islands of pure initiator embedded in undecanethiol. Such segregation of thiols in mixed self-assembled monolayers is well precedented.[42,43] Within each island, initiation efficiency would be constant, and dilution of initiators would simply decrease the number or size of islands. Similar phase separation effects were reported by Ejaz et al. during the co-deposition of a triethoxysilane-terminated initiator (2-(4-chlorosulfonylphenyl)ethyltrimethoxysilane) and *n*-octadecyltrimethoxysilane, an inert diluent.[22] Jordi and Seery used a related approach to anchor norbornene-substituted dimethylethoxysilane initiators to silica nanoparticles for ring opening metathesis polymerization.[44−46] Dilution with trimethylethoxysilane provided surfaces with some control over the initiator density.

This paper describes methods for controlling the density of surface-initiated polymer brushes to create arbitrarily dense arrays of polymers on Au and SiO_2 surfaces. To overcome “island effects” caused by phase separation in self-assembled monolayers (SAMs) of thiols on Au, we first transform the Au surface to an alcohol-terminated monolayer using mercaptoundecanol. Treating this surface with mixtures of α-bromopropionyl bromide and α-methylpropionyl bromide yields active initiators dispersed in a matrix of inactive α-methylpropionate esters. Because the resultant initiator and diluent molecules differ only in the replacement of a bromo group by a methyl group, little phase separation is expected. In the case of SiO_2, we show that obtaining initiator monolayers of known densities requires matching both the reactivity and size of the monochlorosilane initiator and diluent. Polymerization from Au and SiO_2 surfaces yields films whose thickness depends greatly on initiator density when the fraction of initiator in the monolayer drops to <10% so initiation efficiency is high. Moreover, control of the density of PHEMA brushes allows swelling in water that ranges from 85 to 2000%.

Experimental Section

Materials. 10-Undecen-1-yl-2-bromo-2-methyl propionate was prepared using a literature procedure.[6] All other chemicals were purchased from Aldrich and used as received unless noted otherwise. 2,2′-Bipyridine (BPY) was recrystallized from hexane and then sublimed. Triethylamine was distilled from calcium hydride under an argon atmosphere at reduced pressure. Methyl methacrylate (MMA) and 2-hydroxyethyl methacrylate (HEMA) were passed through a 10 cm column of basic alumina to remove inhibitors. After purification, the monomers, solvents, and all liquid chemicals were transferred to Schlenk flasks, degassed using three freeze−pump−thaw cycles, and then transferred into a drybox. Unless otherwise specified, routine ^{1}H NMR (500 MHz) and ^{13}C NMR (125 MHz) spectra were carried out in $CDCl_3$ using a Varian UnityPlus-500 spectrometer with the residual proton signals from the solvent as the chemical shift standard. Mass spectral analyses were carried out on a VG Trio-1 benchtop GC-MS.

Synthesis of 2-Methylpropionyl Bromide (2-MPB) (2). Phosphorus tribromide (15.2 mL, 0.164 mol) was added dropwise to well-stirred isobutyric acid (6.4 mL, 0.068 mol) at 0 °C. After the addition was complete, the reaction was stirred at 0 °C for 3 h and then at room temperature for 15 h. Fractional distillation of the reaction mixture under N_2 gave 2-MPB as a clear liquid in 75% yield; bp 110 °C (lit. bp 107−113 °C). ^{1}H NMR δ: 3.00 (m, 1H, CH), 1.26 (d, 6H, CH_3). ^{13}C NMR δ: 175.0 (C═O), 51.0 (CH), 18.8 (CH_3). EI-MS: $m/z = 151$.

Determination of the Relative Reactivity of 2-Bromopropionyl Bromide (2-BPB, 1) and 2-MPB with Alcohols. Using a literature procedure for the synthesis of the esters as a guide,[5] mixtures of 2-BPB and 2-MPB (various ratios of 2-BPB/2-MPB, 14.8 mmol total) were added by syringe to a well-stirred solution of hexadecanol (2.986 g, 12.34 mmol) in 150 mL of CH_2Cl_2 at 0 °C under N_2. After stirring at 0 °C for 1 h and then at room temperature for 12 h, the mixture was washed with aqueous 2 N sodium carbonate saturated with NH_4Cl. The organic layer was evaporated to dryness, and the crude product was purified by flash chromatography (ethyl acetate/hexane = 1:10). Removal of the solvent gave a colorless oil in quantitative yield. The ratio of two esters in the product was determined using integration of the α-methyl peaks in ^{1}H NMR.

Hexadecyl-2-bromopropanoate. ^{1}H NMR δ: 4.33 (q, 1H, CH), 4.13 (m, 2H, CH_2), 1.79 (d, 3H, CH_3), 1.63 (m, 2H, CH_2), 1.19−1.32 (m, 26H, CH_2), 0.85 (t, 3H, CH_3). ^{13}C NMR δ: 170.2 (C═O), 66.0 (CH_2), 40.2 (CH), 31.9 (CH_2), 29.7 (CH_2), 29.5 (CH_2), 29.4 (CH_2), 29.3 (CH_2), 29.1 (CH_2), 28.4 (CH_2), 25.7 (CH_2), 22.7 (CH_2), 21.6 (CH_3), 14.1 (CH_3). EI-MS: $m/z = 377$.

Hexadecyl-2-methylpropanoate. ^{1}H NMR δ: 4.03 (t, 2H, CH_2), 2.51 (m, 1H, CH), 1.60 (d, 2H, CH_2), 1.17−1.32 (m, 26H, CH_2), 1.14 (d, 6H, 2CH_3), 0.86 (t, 3H, CH_3). ^{13}C NMR δ: 177.2 (C═O), 64.4 (CH_2), 34.0 (CH), 31.9 (CH_2), 29.7 (CH_2), 29.6 (CH_2), 29.5 (CH_2), 29.3 (CH_2), 29.2 (CH_2), 28.7 (CH_2), 25.9 (CH_2), 22.7 (CH_2), 19.0 (CH_3), 14.1 (CH_3). EI-MS: $m/z = 312$.

Synthesis of (11-(2-Bromo-2-methyl)propionyloxy)undecyldimethylchlorosilane (3) and (11-(2,2-Dimethyl)propionyloxy)undecyldimethylchlorosilane (4). 10-Undecen-1-yl-2-bromo-2-methyl propionate[6] (14.4 g, 45.1 mmol) and 49 mL of dimethylchlorosilane (451 mmol) were added to an oven-dried flask. The hydrogen hexachloroplatinate(IV) catalyst was then added (48 mg), and the mixture was stirred at room temperature overnight. The solution was then diluted in toluene and quickly filtered through a 5 cm plug of activated carbon to remove the catalyst. Removal of the solvent under reduced pressure gave 5.80 g of **3** as a colorless oil (31.1%), which was stored in a drybox at 0 °C until used. ^{1}H NMR δ: 4.14 (t, 2H, CH_2), 1.90 (s, 6H, CH_3), 1.65 (m, 2H, CH_2), 1.37−1.24 (m, 16H, CH_2), 0.79 (t, 2H, CH_2), 0.37 (s, 6H, CH_3). ^{13}C NMR δ: 171.69 (C═O), 66.11 (CH_2), 55.95 (CH), 32.92 (CH_2), 29.54 (CH_2), 29.47 (CH_2), 29.42 (CH_2), 29.20 (CH_2), 29.13 (CH_2), 28.30 (CH_2), 25.75 (CH_2), 22.93 (CH_2), 18.94 (CH_3), 1.64 (CH_3).

A similar procedure was used to prepare (**4**) in 68.1% yield. ^{1}H NMR δ: 4.02 (t, 2H, CH_2), 1.59 (m, 2H, CH_2), 1.37−1.24 (m, 16H, CH_2), 1.17 (s, 9H, CH_3), 0.79 (t, 2H, CH_2), 0.37 (s, 6H, CH_3). ^{13}C NMR δ: 178.63 (C=O), 64.43 (CH_2), 38.70 (CH), 32.94 (CH_2), 29.53 (CH_2), 29.47 (CH_2), 29.45 (CH_2), 29.21 (CH_2), 28.59 (CH_2), 27.19 (CH_2), 25.88 (CH_2), 22.95 (CH_2), 18.96 (CH_3), 1.64 (CH_3).

Determination of the Relative Reactivity of Silane Initiator and Diluent with Alcohols. Using a literature procedure for the synthesis of the esters as a guide,[5] an equimolar mixture of initiator **3** and diluent **4** (4 mmol) was added by syringe to a well-stirred solution of hexadecanol (0.847 g, 3.5 mmol) in 15 mL of CH_2Cl_2 at room temperature under N_2 for 24 h. The reaction was quenched by adding 100 mL of saturated aqueous NH_4Cl, and the mixture was extracted with diethyl ether (2 × 100 mL). The combined organic layers were dried over magnesium sulfate, and solvent was removed in vacuo. The ratio of two esters in the product was determined by integrating the corresponding methyl resonances in the ^1H NMR spectrum.

Preparation of Initiator-Modified Au Substrates. Au-coated Si wafers (200 nm of Au sputtered on 20 nm of Cr on Si (100) wafers) were UV/O_3 cleaned for 15 min before use and transferred into a N_2-filled glovebag. A hydroxy-terminated SAM was formed by immersing the Au-coated substrates in a vial containing a 1 mM ethanolic solution of 11-mercapto-1-undecanol (MUD) for 24 h. After removing the vial from the glovebag, the substrates were rinsed sequentially with ethanol and water and then dried under a stream of N_2. The ellipsometric thickness of the MUD layer was 10−15 Å. MUD-coated substrates were transferred to a drybox filled with N_2 and were dipped in a solution of 0.12 M triethylamine in anhydrous THF at ~0 °C. After 1 min, a mixture of 2-BPB and 2-MPB in anhydrous THF (0.1 M) was added dropwise to the solution to achieve initiator immobilization. The reaction time was limited to 2−3 min because thiol-terminated SAMs could be unstable in the presence of acid bromides. After rinsing with THF in the drybox, the Au substrates were removed from the drybox, rinsed with ethyl acetate, ethanol, and Milli-Q water (18 MΩcm) sequentially and dried under a stream of N_2.

Preparation of Initiator-Modified SiO_2 Substrates. UV/O_3-cleaned Si wafers with an ellipsometrically determined oxide thickness of 16 Å were transferred to a drybox filled with N_2 and immersed in a toluene solution (20 mL) containing triethylamine (150 μL) and 30 μL of a mixture of initiator **3** and either diluent **4** or trimethylchlorosilane (TMSCl). (Initiator layers give thicker polymer brushes when they are prepared in solutions containing triethylamine.) After 48 h without stirring, the samples were removed from the solution, placed in fresh toluene, and sonicated for 1 min. Following additional rinsing with toluene, acetone, and ethanol, the substrates were dried under a stream of N_2. The ellipsometric thickness of the initiator layer was ~10 Å.

Surface-initiated polymerizations of MMA. Polymerizations of MMA were carried using a procedure developed by Huck and co-workers as a guide.[41] In an N_2-filled drybox, MMA (10 g, 100 mmol), bipyridine (312 mg, 2.0 mmol), and CuBr (143 mg, 1.0 mmol) were added to a 30 mL scintillation vial containing well-stirred MeOH (8 mL). After removing the vial from the drybox, deionized water (2 mL) was added to the mixture with a syringe, and this vial along with a second vial containing an initiator-modified Au or SiO_2 substrate were transferred into a glovebag filled with N_2. The deionized water was not degassed, and some reaction of Cu(I) with O_2 may yield Cu(II) to help control the polymerization. After stirring the catalyst mixture for an hour, the solution was poured into the vial containing the initiator-modified substrate to initiate polymerization. Following a 0.5−8 h reaction time, the vial was removed from the glovebag, and the substrate was washed sequentially with water, ethyl acetate, ethanol, and water and dried under a stream of N_2.

Surface-Initiated Polymerization of HEMA. The polymerization of HEMA was based on a previously described procedure.[28] In a Schlenk flask, 244 mg (1.56 mmol) of bipyridine was added to 20 mL of an aqueous solution of monomer (HEMA/H_2O, 1:1 v/v). The mixture was stirred until homogeneous and then was degassed using three freeze−pump−thaw cycles. CuCl (55 mg, 0.55 mmol) and $CuBr_2$ (36 mg, 0.16 mmol) were added quickly into the flask under Ar, and this mixture was sonicated for 1 min and transferred into a glovebag filled with N_2. After stirring the catalyst mixture for an hour in the glovebag, the solution was poured into a second vial containing an initiator-covered Au or SiO_2 substrate. The polymerization was allowed to proceed at room temperature for a set reaction time of 0.5−8 h, and then the vial was removed from the glovebag. The substrate was removed from the vial, washed sequentially with water, ethyl acetate, ethanol, and water, and dried under a stream of N_2.

Characterization Methods. Film thicknesses were determined using a rotating analyzer ellipsometer (model M-44; J. A. Woollam) at an incident angle of 75° using 44 wavelengths of light between 414.0 and 736.1 nm. Thickness determinations were performed on at least three spots on each substrate. For films with thicknesses greater than 40 nm, both thickness and refractive index were calculated, while the refractive index of thinner films was usually assumed to be 1.5. (Assuming refractive indices of 1.45 or 1.6 results in thickness changes of only ~10%). For swelling measurements, Au wafers modified with PHEMA brushes were placed in a trapezoidal cell containing glass windows aligned perpendicular to the light beam. After measuring the ellipsometric parameters of the film/substrate in the air-filled cell, the cell was filled with deionized water. Two min later, ellipsometric measurements were performed on the swollen films immersed in water. The optical constants of water were obtained from literature data,[47] and the refractive indices determined for the swollen films reflected the approximate volume fractions of water (refractive index around 1.333) and polymer (refractive index of 1.5) in the film. For example, films with swollen thicknesses suggesting a composition of ~95% water had refractive indices around 1.334, while films containing 50% water had refractive indices around 1.416. Reflectance FTIR spectroscopy was performed using a Nicolet Magna-IR 560 spectrometer containing a PIKE grazing angle (80°) attachment.

Results and Discussion

Preparation of Au Substrates with Controlled Initiator Densities. Our strategy for controlling the areal density of chains in polymer brushes is to vary the concentration of the immobilized ATRP initiators from which they grow. Scheme 1 outlines the synthetic pathway for anchoring initiators on sputtered Au substrates and controlling their density. We first generate an alcohol-terminated SAM and then react the terminal hydroxy groups with a mixture of 2-BPB and 2-MPB to obtain ATRP initiators (α-bromoesters) dispersed among inert diluent molecules (α-methylesters). The reaction of 2-BPB and 2-MPB with the surface hydroxy groups should be nonselective because the two acyl bromides are similar in terms of their steric demands. To verify that these molecules have similar reactivities, we carried out a competitive reaction of 2-BPB and 2-MPB with hexadecanol in CH_2Cl_2. As expected, ^1H NMR analysis of the reaction products showed essentially identical reactivities for the two acyl bromides (Figure S1, Supporting Information). We assume that the lack of selectivity shown in solution will also occur for reactions with the hydroxy-terminated SAM and that the surface composition will mirror the ratio of 2-BPB and 2-MPB used to derivatize the monolayer. Moreover, self-organization processes that might lead to phase separation in the film should be insignificant because a 3 min reaction time is sufficient to anchor acyl bromides to the surface, and the size and hydrophobicity of the initiator and diluent are very similar. The appearance of a carbonyl peak (1743 cm^{-1}) in reflectance FTIR spectra of derivatized monolayers confirmed reaction of the surface with the acid bromides (Figure S2), but it could not provide a ratio of initiator to diluent in these films because both molecules contain ester groups.

Polymerization of MMA and HEMA from Au Substrates with Controlled Initiator Densities. PMMA brushes were

Scheme 1. Polymerization of Methyl Methacrylate (MMA) from Diluted-Initiator Monolayers on Au Substrates

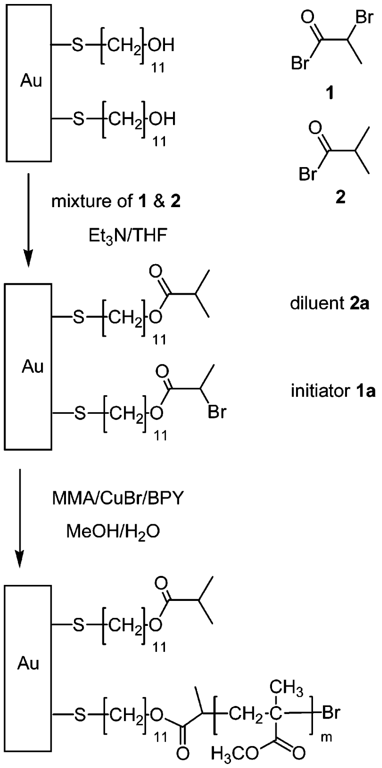

grown from Au substrates with initiator densities ranging from 100% to 1% 2-BPB by immersing the substrates in water/methanol solutions containing an ATRP catalyst system and monomer. These polymerization conditions are comparable to those used by Huck et al. in their initiator density studies.[41] Preliminary AFM imaging of the films show no significant morphological differences as a function of initiator density. Figure 1 shows ellipsometric thicknesses for MMA brushes grown from Au substrates modified with different initiator densities. Consistent with previous studies of this catalyst system using 100% initiator, all of the initiator concentrations yielded a near-linear increase in film thickness as a function of time, indicating that the polymerization is controlled. If termination and chain transfer are unimportant, the film growth rate (slopes in Figure 1) should be proportional to the density of initiation sites. The data in Figure 2 and Table 1 clearly show that the dependence of growth rate on initiator concentration is more complicated than this. The polymerization rate is nearly constant (7−9 nm/hr) from substrates with 25−100% 2-BPB and then decreases with further dilution to 1.5 nm/hr for 1% 2-BPB. FTIR and ellipsometric data show no evidence for polymer growth from a control surface with 0% 2-BPB. The most likely reason for the nonlinear relationship between film growth rate and initiator concentration is bimolecular termination. Initiators on flat surfaces are localized in a plane, and because their effective concentration is very high, we expect that radical recombination near the surface should be facile early in the polymerization. (After the initial rapid radical combination, termination must slow dramatically to allow for a constant growth rate.) This picture is in accord with earlier results that showed that about 1 out of 10 initiators successfully grow high-molecular-weight polymers from flat surfaces.[20] Thus, the dependence of the film growth rate on initiator coverage should be weak until initiator concentration decreases to 10%, and this is consistent with the data in Table 1.

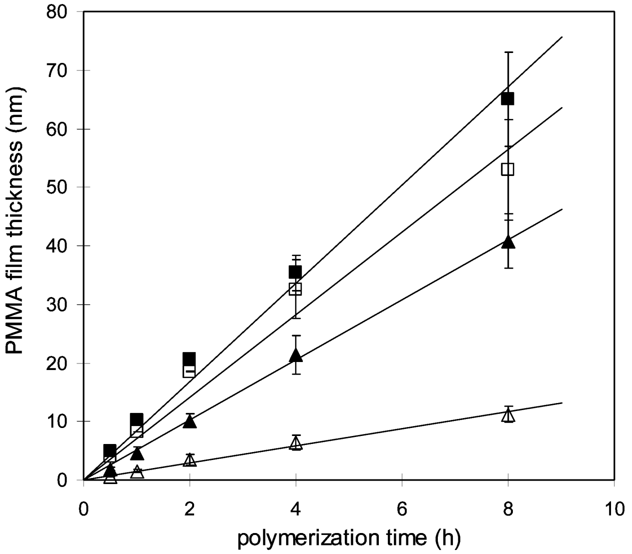

Figure 1. Evolution of the ellipsometric brush thickness with time for the polymerization of MMA (methyl methacrylate) from diluted-initiator monolayers on Au substrates at 28 °C. (□, 100% 2-bromopropionyl bromide (2-BPB); ■, 50% 2-BPB; ▲, 5% 2-BPB; △, 1% 2-BPB). Polymerization conditions: [MMA] = 5 M, [CuBr] = 0.05 M, [2,2′-bipyridine] = 0.1 M, in 10 mL of 4:1 (v/v) $MeOH/H_2O$. The points are the average of data from two independent runs, and the limits of the error bars are the measured film thicknesses from the two runs. The lines are least-squares fit to the data constrained to intersect the origin.

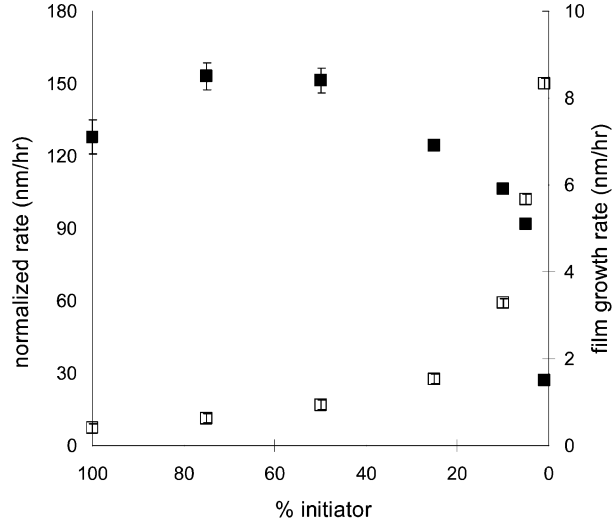

Figure 2. Film growth rate (■) and normalized polymerization rate (□) (observed film growth rate/fractional coverage of the surface by initiator) in surface-initiated polymerization of MMA (methyl methacrylate) from diluted-initiator monolayers on Au substrates. The polymerization conditions are described in Figure 1.The error bars are derived from the standard deviations calculated from the linear fits to the data in Figure 1.

Polymerization of HEMA from Au (Figures 3 and 4, Table 2) shows similar trends. The relatively constant rate of film growth again suggests a controlled polymerization on this surface, and relative to films grown from surfaces with 100% initiator, thickness decreases 6-fold for films grown from monolayers with 1% initiator.

Polymerization of MMA and HEMA from SiO_2 Substrates with Controlled Initiator Densities. In the case of SiO_2 surfaces, we controlled initiator density through silanization with mixtures of the two monochlorosilanes shown in Scheme 2. We utilized monochloroalkylsilanes rather than trichloroalkylsilane because polymerization of tricholoralkylsilanes in the presence

Table 1. Methyl Methacrylate Polymerization Rates from Au Substrates at Various Initiator Densities[a]

initiator composition[b] (% 2-BPB)	initiator density[c] (initiators/nm^2)	PMMA thickness at 8 h (nm)	film growth rate[d] (nm/hr)	normalize rate[e] (nm/hr)
100	4	53	7.1 ± 0.4	7.1 ± 0.4
75	3	69	8.5 ± 0.3	11.3 ± 0.4
50	2	65	8.4 ± 0.3	16.8 ± 0.6
25	1	55	6.9 ± 0.1	27.6 ± 0.2
10	0.4	47	5.9 ± 0.1	59 ± 1.2
5	0.2	41	5.1 ± 0.1	102 ± 1.4
1	0.04	11	1.5 ± 0.1	150 ± 5.0

[a] Conditions for the polymerization are described in Figure 1. [b] Based on the ratio of 2-bromopropionyl bromide (2-BPB) and 2-methylpropionyl bromide (2-MPB) used in the anchoring step. [c] Assuming full coverage = 4 sites/nm^2.[48] [d] Defined as the slope of the line defined by least-squares fits to the data in Figure 1. The errors are the standard deviations derived from the linear fits to the data. [e] Defined as the film growth rate divided by fractional coverage of the surface by initiator.

Table 2. 2-Hydroxyethyl Methacrylate Polymerization Rates from Au Substrates at Various Initiator Densities[a]

initiator composition[b] (% 2-BPB)	initiator density[c] (initiators/nm^2)	PHEMA thickness at 8 h (nm)	film growth rate[d] (nm/hr)	normalized rate[e] (nm/hr)
100	4	128	16.2 ± 0.3	16.2 ± 0.3
50	2	133	16.0 ± 0.8	32.0 ± 1.5
5	0.2	84	10.6 ± 0.3	212 ± 5.2
1	0.04	22	2.8 ± 0.2	280 ± 16
0.1	0.004	1.5	0.20 ± 0.02	190 ± 20

[a] Conditions for the polymerizations are described in Figure 3. [b] Based on the ratio of 2-bromopropionyl bromide (2-BPB) and 2-methylpropionyl bromide (2-MPB) used in the anchoring step. [c] Assuming full coverage = 4 sites/nm^2.[48] [d] Defined as the slope of the line defined by least-squares fits to the data in Figure 3. The errors are the standard deviations derived from the linear fits to the data. [e] Defined as the film growth rate divided by fractional coverage of the surface by initiator.

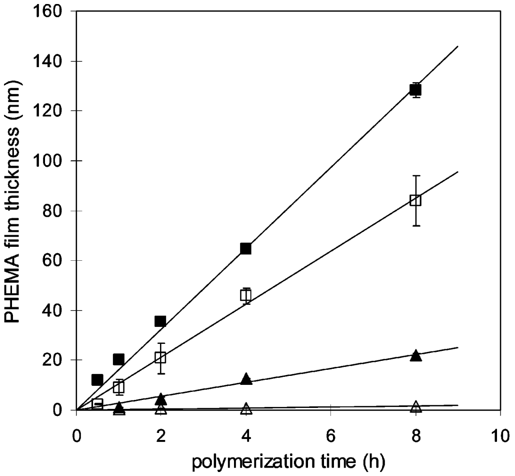

Figure 3. Evolution of the ellipsometric brush thickness with time for the polymerization of 2-hydroxyethyl methacrylate (HEMA) from diluted-initiator monolayers on Au substrates at 28 °C. (■, 100% 2-bromopropionyl bromide (2-BPB); □, 5% 2-BPB; ▲, 1% 2-BPB; △, 0.1% 2-BPB). Polymerization conditions: [CuCl] = 27.5 mM, [CuBr$_2$] = 8.0 mM, [2,2′-bipyridine] = 78 mM, in 20 mL of a 1:1 (v/v) mixture of HEMA and H_2O ([HEMA] = 4 M). The points are the average of data from two independent runs, and the limits of the error bars are the measured film thicknesses from the two runs. The lines are a least-squares fit to the data constrained to intersect the origin.

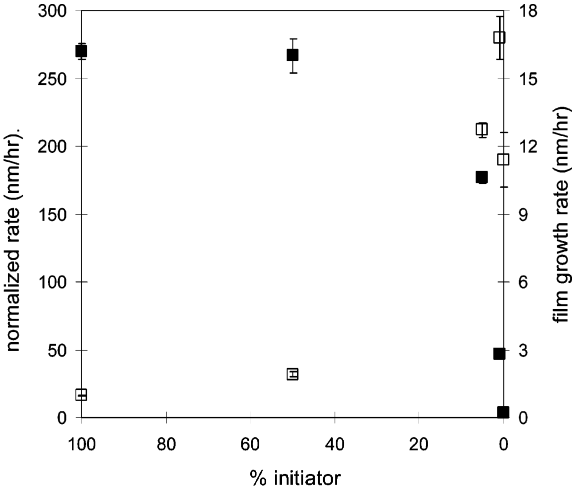

Figure 4. Film growth rate (■) and normalized polymerization rate (□) (observed film growth rate/fractional coverage of the surface by initiator) in surface-initiated polymerization of 2-hydroxyethyl methacrylate (HEMA) from diluted-initiator monolayers on Au substrates. The polymerization conditions are described in Figure 3. The error bars are derived from the standard deviations calculated from the linear fits to the data in Figure 3.

of trace amounts of water gives rise to a number of possible surface structures.[49] The monochloroalkylsilanes, **3** and **4**, are structurally similar, but one is an α-bromoester capable of initiating ATRP, while the second contains an inert methylester. Reactions of **3** and **4** with hydroxy groups in solution show that their reactivities are indistinguishable, and based on their similar sizes and shapes, we expect that their reactivities toward hydroxy-terminated surfaces should also be identical. Thus, the composition of a silane monolayer should accurately reflect the molar ratio of **3** and **4** in the solution used to modify the surface.

Polymerization of HEMA on SiO_2 yielded results that are similar, though not identical, to polymerization on Au, as shown in Figure 5. However, the polymerization rates for MMA and HEMA were consistently lower on Au than SiO_2. We recently observed that PMMA blocks initiated from a brush on gold grew faster than PMMA grown directly from initiators anchored to a Au surface, suggesting radical quenching by the gold surface. The rate of polymerization from initiators on SiO_2 decreased >30-fold on going from 100% to 1% initiator, but in this case, the polymerization rate decreased monotonically as a function of initiator packing density (Figure 6). An important difference between Au and SiO_2 surfaces is the number and density of sites available on the surface for binding initiator. Studies of anchoring octadecyldimethylsilyl chlorides to a variety of silica surfaces[50] indicate a limiting area/molecule of 0.6 nm^2, with typical values of ~0.65 nm^2 or ~1.54 chains/nm^2. Because this represents an areal density roughly 40% of that for a SAM on Au, the same initiator/diluent ratio applied to Au and SiO_2 will

Scheme 2. Polymerization of 2-hydroxyethyl methacrylate (HEMA) from Diluted-Initiator Monolayers on SiO_2 Substrates

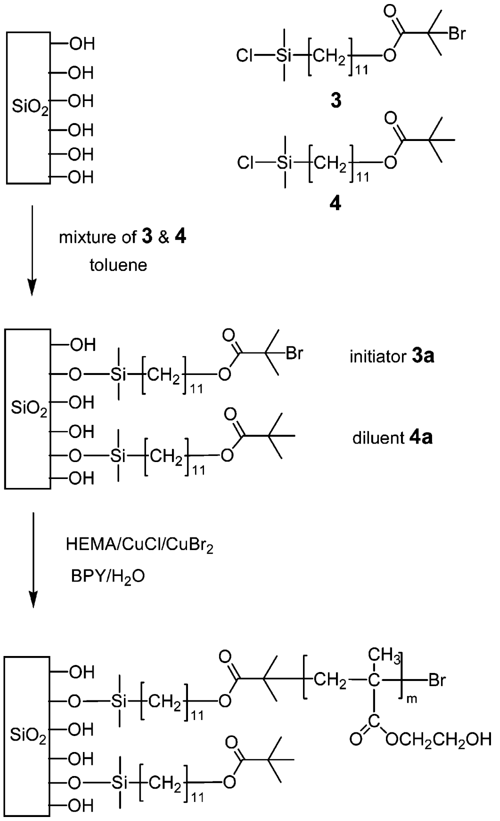

yield a larger average distance between initiators on SiO_2. When the data are normalized on the basis of area/initiator, the polymerization rates from Au and Si are similar when the initiator is diluted to <10%, using the Au surface as the reference. More concentrated initiator layers show distinctly different behavior for SiO_2 and Au surfaces. HEMA polymerization rates from SiO_2 increase with initiator concentration, but the rates from Au are nearly constant.

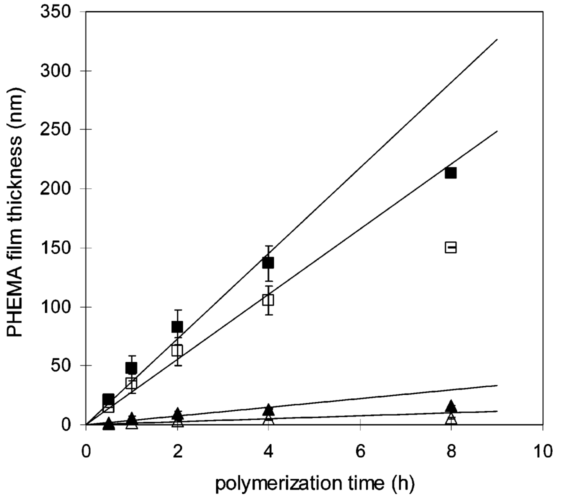

Figure 5. Evolution of the ellipsometric brush thickness with time for the polymerization of 2-hydroxyethyl methacrylate (HEMA) from diluted-initiator monolayers on SiO_2 substrates at 28 °C. (■, 100% **3**; □, 50% **3**; ▲, 5% **3**; △ 1% **3**). Polymerization conditions: [CuCl] = 27.5 mM, [$CuBr_2$] = 8.0 mM, [2,2′-bipyridine] = 78 mM, in 20 mL of a 1:1 (v/v) mixture of HEMA and H_2O ([HEMA] = 4 M). The points are the average of data from two independent runs, and the limits of the error bars are the measured film thicknesses from the two runs. The lines are a least-squares fit to the 0−4 h data, constrained to intersect the origin.

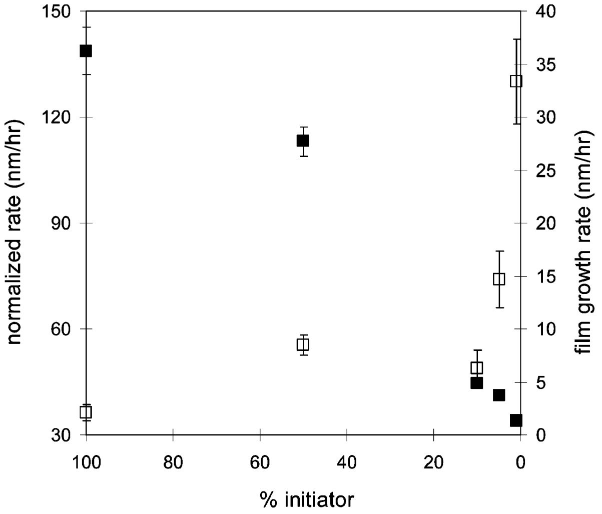

Figure 6. Film growth rate (■) and normalized polymerization rate (□) (observed film growth rate/fractional coverage of the surface by initiator) in surface-initiated polymerization of 2-hydroxyethyl methacrylate (HEMA) from diluted-initiator monolayers on SiO_2 substrates. The polymerization conditions are described in Figure 5. The error bars are derived from the standard deviations calculated from the linear fits to the data in Figure 5. Film growth rates and normalized rates appear in Table S1.

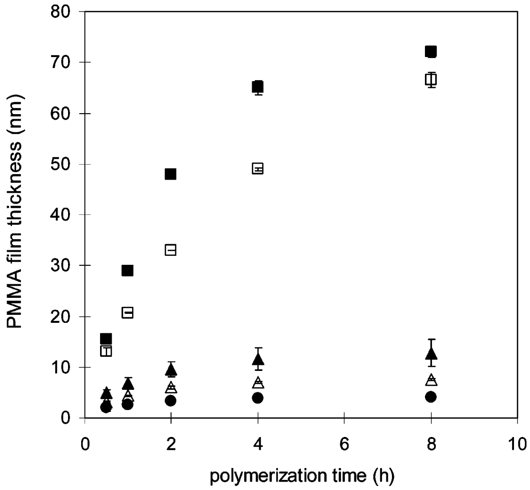

Figure 7. Evolution of the ellipsometric brush thickness with time for the polymerization of methyl methacrylate (MMA) from diluted-initiator monolayers on SiO_2 at 28 °C (■, 100% **3**; □, 50% **3**; ▲, 10% **3**; △, 5% **3**; ●, 1% **3**). Polymerization conditions: [MMA] = 5 M, [CuBr] = 0.05 M, [2,2′-bipyridine] = 0.1 M, in 20 mL of 4:1 (v/v) $MeOH/H_2O$. The points are the average of data from two independent runs, and the limits of the error bars are the measured film thicknesses from the two runs.

The rate of polymerization of MMA on SiO_2 also decreased as a function of initiator packing density (>20-fold from 100% to1% initiator), but the decrease in growth rate with time (nonlinearity in Figure 7) suggests that there is significantly more termination with this system than on Au. However, like the Au-based system, these data clearly show that decreasing the initiator density below a threshold value results in dramatic increases in the normalized polymerization rate. Because the same pattern is seen for HEMA and MMA polymerizations, we speculate that the difference in the polymerization rates at high initiator concentrations on SiO_2 and Au is related to the decreased chain density on SiO_2 surfaces. A reasonable question is whether the sizes and shapes of initiator and diluent need to be matched for effective control of initiator density on SiO_2. Unlike SAMs on Au, the reaction of a chlorosilane with silanols

Table 3. Aqueous Swelling of Poly(2-hydroxyethyl methacrylate) (PHEMA) Brushes on Au Substrates[a]

initiator composition[b] (% 2-BPB)	PHEMA film thickness in air[c] (nm)	PHEMA film thickness in water[d] (nm)	% increase in thickness
100	43	77	77
50	38	62	62
5	47	83	76
1	17	45	180
0.1	4.2	75	1600

[a] Average film thicknesses based on two data sets. [b] Based on the ratio of 2-bromo propionyl bromide (2-BPB) and 2-methylpropionyl bromide (2-MPB) used in the anchoring step. [c] Obtained using 1.5 as the film refractive index. [d] Both film thickness and refractive index were obtained from fits to ellipsometric data.

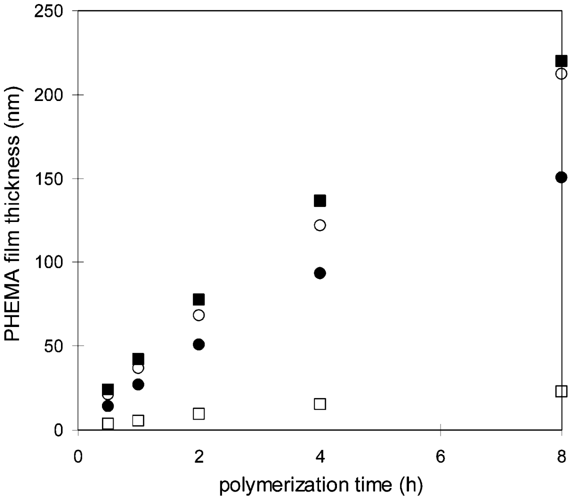

Figure 8. Evolution of the ellipsometric brush thickness with time for the polymerization of 2-hydroxyethyl methacrylate (HEMA) from diluted-initiator monolayers on SiO_2 at 28 °C. (○, 100% **3**; ●, 50% **3**, diluted with **4**; ■, 100% **3**; □, 50% **3**, diluted with trimethylsilyl chloride). The two data sets (squares and circles) are from independent runs, and the two 100% initiator runs show the repeatability of the data. The conditions used for the experiments are identical to those of Figure 5.

on SiO_2 substrates forms covalent Si−O bonds and phase separation on SiO_2 surfaces is very slow.[51]

To test for size effects in the anchoring process, we prepared two 50% initiator layers, one using diluent **4** and a second where trimethylsilyl chloride substituted for **4**. Trimethylsilyl chloride should have the same chemical reactivity as **4**, and its cross-sectional area at SiO_2 should also be similar. Polymerizations were carried out from 50% initiator layers, one diluted with trimethylsilyl chloride and the other with **4**. Polymerizations from substrates with 100% initiator were run concurrently with each 50%-initiator substrate, enabling direct comparison of the growth rates from the two initiator dilution schemes. As shown in Table S1 and Figure 8, substrates where the initiators were diluted to 50% with **4** have HEMA polymerization rates $\sim{}^2/_3$ of those from 100% **3**. In contrast, polymerization rates decreased to $^1/_6$ of the 100% control when trimethylsilyl chloride was used as the diluent, and we conclude that *the chain length on the diluent does matter*. (The polymerization rates for the two 100% control samples differed by less than 10%). We think that initially, both initiator and diluent have equal access to the surface and deposit homogeneously. However, as the surface is increasingly covered, initiators screen adjacent silanols and the shorter trimethylsilyl chloride competes more efficiently than **3** for surface silanols, resulting in lower than expected initiator densities and film growth rates. Thus, simply using the same functional group for anchoring initiator and diluent cannot guarantee homogeneous dilution of initiators on SiO_2 and other substrates.

Aqueous Swelling of PHEMA Films Grown from Au Substrates. All of the data presented thus far suggest that films prepared from 100% initiator should have much higher chain densities than films prepared from 1% initiators. Lower chain densities should result in greater swelling when films are exposed to a good solvent because the chains in the less dense film will likely be less extended prior to exposure to solvent. We examined the swelling of PHEMA in water, and the results are shown in Table 3 and Figure S3. Percent swelling increases from 85% to 1600% when using films prepared from 0.1% rather than 100% initiator. We should note that swelling of PHEMA chains in water is complicated by the fact that PHEMA films grown from a surface are probably lightly cross-linked. At lower initiation densities, both lower cross-linking and lower chain densities could lead to an increase in swelling. Moreover, the extremely high swelling at 0.1% should be viewed with caution because the refractive index of the film is nearly the same as that of the ambient water, making a thickness determination by ellipsometry difficult. Nonetheless, these data clearly show that film density can have a dramatic effect on physical properties.

Conclusions

In conclusion, we have prepared Au and SiO_2 substrates with various immobilized initiator densities using systems that should lead to a homogeneous distribution of initiator on the surface. Changes in the polymerization rate as a function of initiator density are consistent with both a decrease in bimolecular termination as the initiator density decreases and a decrease in the number of chains on the surface when the initiator density drops below 10% on Au. Finally, decreases in chain density lead to increases in film swelling in a good solvent, probably because chains are less extended prior to exposure to solvent when they are less dense. Future studies will examine the immobilization of macromolecules in polymer brushes as a function of film density.

Acknowledgment. We thank the Center for Sensor Materials, an NSF MRSEC at Michigan State University, for financial support of this work. M.L.B. acknowledges funding from NSF grant CHE-0316244.

Supporting Information Available: HEMA polymerization rates from silicon substrates at various initiator densities (Table S1), HEMA polymerization rates from silicon substrates using trimethylsilyl chloride and (11-(2,2-dimethyl)propionyloxy)undecyldimethylchlorosilane as diluents (Table S2), ^1H NMR data for the reaction of 2-BPB and 2-MPB with hexadecanol (Figure S1), FTIR spectra of diluted-initiator monolayers on Au substrates (Figure S2), and aqueous swelling data for HEMA brushes grown from diluted-initiator monolayers (Figure S3). This material is available free of charge via the Internet at http://pubs.acs.org.

References and Notes

(1) Huang, X.; Doneski, L. J.; Wirth, M. J. *Anal. Chem.* **1998**, *70*, 4023−4029.

(2) Zhao, B.; Brittain, W. J. *Prog. Polym. Sci.* **2000**, *25*, 677–710.
(3) Edmondson, S.; Osborne, V. L.; Huck, W. T. S. *Chem. Soc. Rev.* **2004**, *33*, 14–22.
(4) Pyun, J.; Kowalewski, T.; Matyjaszewski, K. *Macromol. Rapid Commun.* **2003**, *24*, 1043–1059.
(5) Shah, R. R.; Merreceyes, D.; Husemann, M.; Rees, I.; Abbott, N. L.; Hawker, C. J.; Hedrick, J. L. *Macromolecules* **2000**, *33*, 597–605.
(6) Matyjaszewski, K.; Miller, P. J.; Shukla, N.; Immaraporn, B.; Gelman, A.; Luokala, B. B.; Siclovan, T. M.; Kickelbick, G.; Vallant, T.; Hoffmann, H.; Pakula, T. *Macromolecules* **1999**, *32*, 8716–8724.
(7) Husseman, M.; Malmstrom, E. E.; McNamara, M.; Mate, M.; Mecerreyes, D.; Benoit, D. G.; Hedrick, J. L.; Mansky, P.; Huang, E.; Russell, T. P.; Hawker, C. J. *Macromolecules* **1999**, *32*, 1424–1431.
(8) Huang, X.; Wirth, M. J. *Macromolecules* **1999**, *32*, 1694–1696.
(9) Ejaz, M.; Yamamoto, S.; Ohno, K.; Tsujii, Y.; Fukuda, T. *Macromolecules* **1998**, *31*, 5934–5936.
(10) von Werne, T.; Patten, T. E. *J. Am. Chem. Soc.* **2001**, *123*, 7497–7505.
(11) Currie, E. P. K.; Norde, W.; Stuart, M. A. C. *Adv. Colloid Interface Sci.* **2003**, *100*, 205–265.
(12) Ionov, L.; Minko, S.; Stamm, M.; Gohy, J. F.; Jerome, R.; Scholl, A. *J. Am. Chem. Soc.* **2003**, *125*, 8302–8306.
(13) Luzinov, I.; Minko, S.; Tsukruk, V. V. *Prog. Polym. Sci.* **2004**, *29*, 635–698.
(14) Minko, S.; Luzinov, I.; Luchnikov, V.; Muller, M.; Patil, S.; Stamm, M. *Macromolecules* **2003**, *36*, 7268–7279.
(15) Zhao, B.; Brittain, W. J. *J. Am. Chem. Soc.* **1999**, *121*, 3557–3558.
(16) Boyes, S. G.; Brittain, W. J.; Weng, X.; Cheng, S. Z. D. *Macromolecules* **2002**, *35*, 4960–4967.
(17) Zhao, B.; Brittain, W. J. *Macromolecules* **2000**, *33*, 342–348.
(18) Rühe, J.; Knoll, N. *J. Macromol. Sci., Polym. Rev.* **2002**, *C42*, 91–138.
(19) Pyun, J.; Matyjaszewski, K. *Chem. Mater.* **2001**, *13*, 3436–3448.
(20) Kim, J. B.; Bruening, M. L.; Baker, G. L. *J. Am. Chem. Soc.* **2000**, *122*, 7616–7617.
(21) Zhao, B.; Brittain, W. J. *Macromolecules* **2000**, *33*, 8813–8820.
(22) Ejaz, M.; Ohno, K.; Tsujii, Y.; Fukuda, T. *Macromolecules* **2000**, *33*, 2870–2874.
(23) Husemann, M.; Mecerreyes, D.; Hawker, C. J.; Hedrick, J. L.; Shah, R.; Abbott, N. L. *Angew. Chem., Int. Ed.* **1999**, *38*, 647–649.
(24) Huang, W.-X.; Baker, G. L.; Bruening, M. L. *Angew. Chem., Int. Ed.* **2001**, *40*, 1510–1512.
(25) Von Werne, T.; Patten, T. E. *J. Am. Chem. Soc.* **1999**, *121*, 7409–7410.
(26) Bantz, M. R.; Brantley, E. L.; Weinstein, R. D.; Moriarty, J.; Jennings, G. K. *J. Phys. Chem. B* **2004**, *108*, 9787–9794.
(27) Brantley, E. L.; Jennings, G. K. *Macromolecules* **2004**, *37*, 1476–1483.
(28) Huang, W.; Kim, J.-B.; Bruening, M. L.; Baker, G. L. *Macromolecules* **2002**, *35*, 1175–1179.
(29) Zhou, F.; Liu, W. M.; Hao, J. C.; Xu, T.; Chen, M.; Xue, Q. J. *Adv. Funct. Mater.* **2003**, *13*, 938–942.
(30) Zhou, F.; Jiang, L.; Liu, W. M.; Xue, Q. J. *Macromol. Rapid Commun.* **2004**, *25*, 1979–1983.
(31) Kaholek, M.; Lee, W. K.; LaMattina, B.; Caster, K. C.; Zauscher, S. *Nano Lett.* **2004**, *4*, 373–376.
(32) Kaholek, M.; Lee, W. K.; Ahn, S. J.; Ma, H. W.; Caster, K. C.; LaMattina, B.; Zauscher, S. *Chem. Mater.* **2004**, *16*, 3688–3696.
(33) von Werne, T. A.; Germack, D. S.; Hagberg, E. C.; Sheares, V. V.; Hawker, C. J.; Carter, K. R. *J. Am. Chem. Soc.* **2003**, *125*, 3831–3838.
(34) Kim, J.-B.; Huang, W.; Wang, C. L.; Bruening, M. L.; Baker, G. L. Bottle Brush Brushes: Ring-Opening Polymerization of Lactide from Poly(hydroxyethyl methacrylate) Surfaces. In *Polymer Brushes*, R. C. Advincula, W. B., Caster, K., Rühe, J., Eds.; Wiley-VCH: New York, 2004; pp 105–117.
(35) Wu, T.; Efimenko, K.; Genzer, J. *J. Am. Chem. Soc.* **2002**, *124*, 9394–9395.
(36) Wu, T.; Efimenko, K.; Vlcek, P.; Subr, V.; Genzer, J. *Macromolecules* **2003**, *36*, 2448–2453.
(37) Liu, Y.; Klep, V.; Zdyrko, B.; Luzinov, I. *Langmuir* **2004**, *20*, 6710–6718.
(38) Wang, X.; Tu, H.; Braun, P. V.; Bohn, P. W. *Langmuir* **2006**, *22*, 817–823.
(39) Tsujii, Y.; Ejaz, M.; Yamamoto, S.; Fukuda, T.; Shigeto, K.; Mibu, K.; Shinjo, T. *Polymer* **2002**, *43*, 3837–3841.
(40) Yamamoto, S.; Tsujii, Y.; Fukuda, T. *Macromolecules* **2002**, *35*, 6077–6079.
(41) Jones, D. M.; Brown, A. A.; Huck, W. T. S. *Langmuir* **2002**, *18*, 1265–1269.
(42) Tamada, K.; Hara, M.; Sasabe, H.; Knoll, W. *Langmuir* **1997**, *13*, 1558–1566.
(43) Bain, C. D.; Evall, J.; Whitesides, G. M. *J. Am. Chem. Soc.* **1989**, *111*, 7155–7164.
(44) Jordi, M. A.; Seery, T. A. P. *J. Am. Chem. Soc.* **2005**, *127*, 4416.
(45) Fissekis, J. D.; Skinner, C. G.; Shive, W. *J. Am. Chem. Soc.* **1959**, *81*, 2715–2718.
(46) Sakurai, S. *J. Biochem.* **1958**, *45*, 379–385.
(47) Harvey, A. H.; Gallagher, J. S.; Sengers, J. *J. Phys. Chem. Ref. Data* **1998**, *27*, 761–774.
(48) Ulman, A.; Eilers, J. E.; Tillman, N. *Langmuir* **1989**, *5*, 1147–1152.
(49) Fadeev, A. Y.; McCarthy, T. J. *Langmuir* **2000**, *16*, 7268–7274.
(50) Sander, L. C.; Wise, S. A. *J. Chromatogr.* **1984**, *163–181*, 163.
(51) Wang, H. B.; Harris, J. M. *J. Am. Chem. Soc.* **1994**, *116*, 5754–5761.

MA060095A